

Application of Bayesian Inversion to Characterization of EDZ

Pavel Exner

2022

0.1 Forward hydro-mechanical model

Let us consider the geometry as a 2D manifold in arbitrary 3D space.

0.1.1 Governing equations

Mechanical model. Deformation of the porous media is modelled by the stationary linear elasticity equation

$$-\operatorname{div}(\sigma(\mathbf{u})) = \mathbf{f} + \mathbf{f}_H. \quad (1)$$

Here \mathbf{u} [m] is the displacement vector field with 3 components, the stress tensor is given by the Hooke law

$$\sigma(\mathbf{u}) = \mathbb{C}\varepsilon(\mathbf{u}) = 2\mu\varepsilon(\mathbf{u}) + \lambda(\mathbb{I} : \varepsilon(\mathbf{u}))\mathbb{I}, \quad (2)$$

and the Lamé parameters are determined in terms of the Young modulus E [Pa] and Poisson's ratio ν [-]:

$$\mu = \frac{E}{2(1+\nu)}, \quad \lambda = \frac{E\nu}{(1+\nu)(1-2\nu)}. \quad (3)$$

The strain tensor in Ω is defined as follows:

$$\varepsilon(\mathbf{u}) = \frac{1}{2}(\nabla\mathbf{u} + \nabla\mathbf{u}^\top). \quad (4)$$

The symbol \mathbf{f} stands for the body load [$\text{N} \cdot \text{m}^{-3}$] and \mathbf{f}_H plays a role in the hydro-mechanical coupling, see (7).

Flow model. We consider the Darcy's law for flow in porous media in the form

$$\mathbf{q} = -\delta\mathbb{K}\nabla h, \quad (5)$$

where \mathbb{K} [$\text{m} \cdot \text{s}^{-1}$] is the hydraulic conductivity tensor, h [m] is the hydraulic pressure head and δ [m] is the thickness of the 2D domain.

The continuity equation for saturated porous medium then takes the form

$$\partial_t(\delta S_s h) + \operatorname{div} \mathbf{q} = F + F_M. \quad (6)$$

where S_s [m^{-1}] is the specific storage and F [$\text{m} \cdot \text{s}^{-1}$] is the source term. The extra source term F_M [$\text{m} \cdot \text{s}^{-1}$] due to mechanics is defined later by (8). In our setting the principal unknowns of the system (5) and (6) are both h and \mathbf{q} (discretization using Lumped Mixed Hybrid Method).

Hydro-mechanical coupling. The mechanics equation (1) is coupled to flow by the term

$$\mathbf{f}_H = -\nabla(\delta\alpha p), \quad p = \varrho_l gh, \quad (7)$$

where p [Pa] is the pressure, α [-] is the Biot coefficient, ϱ_l [$\text{kg} \cdot \text{m}^{-3}$] is the fluid density and g [$\text{m} \cdot \text{s}^{-2}$] is the gravitational acceleration. Conversely, the deformation affects the flow via the additional term

$$F_M = -\partial_t(\delta\alpha \operatorname{div} \mathbf{u}) \quad (8)$$

on the right hand side of (6). The numerical solution of coupled hydro-mechanical problems is solved by an iterative splitting, where in order to achieve convergence the flow equation is modified as follows:

$$\partial_t(\delta(S + S_{extra}) h) + \operatorname{div} \mathbf{q} = F + F_M + \partial_t(\delta S_{extra} h_{old}). \quad (9)$$

Here h_{old} is the previous value of piezometric head in the iteration process and S_{extra} is an extra storativity coefficient whose value affects the rate of convergence.

0.1.2 Forward Model 1 – simplest setting

We list the common values of the elementary parameters, i.e. fluid density, gravitational acceleration and 2D domain cross-section:

$$\rho_l = 1000 \text{ kg} \cdot \text{m}^{-3}, g = 9.81 \text{ m} \cdot \text{s}^{-2} \text{ and } \delta = 1 \text{ m.}$$

The geometry is shown in Figure 1 and boundary conditions are depicted. The input parameters of the fixed forward model are gathered in Table 1.

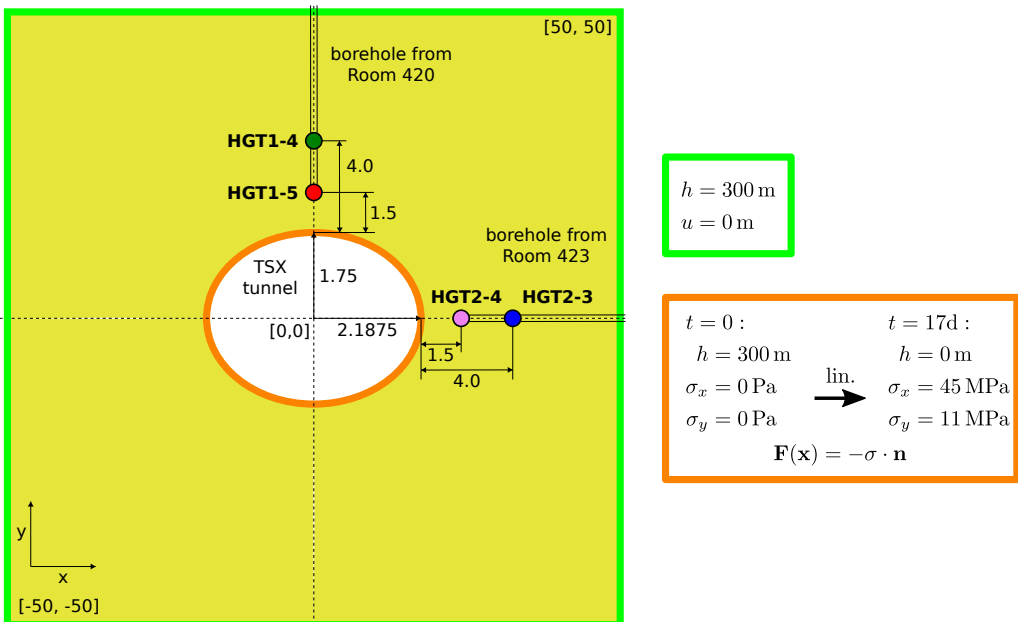


Figure 1: Model geometry of the tunnel 2D cross-section with boundary condition depicted.

The excavation during first 17 days is simulated through the inner boundary condition on the tunnel surface. Pressure head is linearly decreased from the initial pressure head to zero (atmospheric pressure head after excavation). The mechanical stress change during excavation is provided by linear increase of stress to the value of the initial stress (there is no supporting material in the tunnel area after excavation).

parameter	symbol	value	unit
hydraulic conductivity	K	$5.886 \cdot 10^{-15}$	$\text{m} \cdot \text{s}^{-1}$
storativity	S	$7.291 \cdot 10^{-8}$	m^{-1}
initial pressure head	h_0	300	m
Biot-Willis coefficient	α	0.2	—
Young modulus	E	$6 \cdot 10^{10}$	Pa
Poisson ratio	ν	0.2	—

Table 1: Forward model input parameters.

Hydraulic conductivity depends on permeability k , dynamic viscozity $\mu = 0.001 \text{ [Pa} \cdot \text{s]}$, fluid density and gravity

$$K = \frac{k\rho_l g}{\mu} \approx 5.886 \cdot 10^{-15} \text{ m} \cdot \text{s}^{-1} \text{ for } k = 6 \cdot 10^{-22} \text{ m}^2. \quad (10)$$

Storativity $S [-]$ depends on the following quantities

$$S = \delta S_s = \delta \rho g (\beta_s + \eta \beta_w) \quad (11)$$

where $\eta [-]$ is porosity, $\beta_w [\text{Pa}^{-1}]$ compressibility of fluid phase and $\beta_s [\text{Pa}^{-1}]$ **PE: compressibility of solid grains** of porous media which can be derived

$$\beta_s = \frac{(\alpha - \eta)(1 - \alpha)}{K} \quad (12)$$

By substituting parameters from Table 1, we get

$$S = 9.81 \cdot 10^3 ((0.2 - 0.007)(1 - 0.2) \cdot 3 \cdot 10^{-11} + 7 \cdot 10^{-3} \cdot 4 \cdot 10^{-10}) \approx 7.291 \cdot 10^{-8} \quad (13)$$

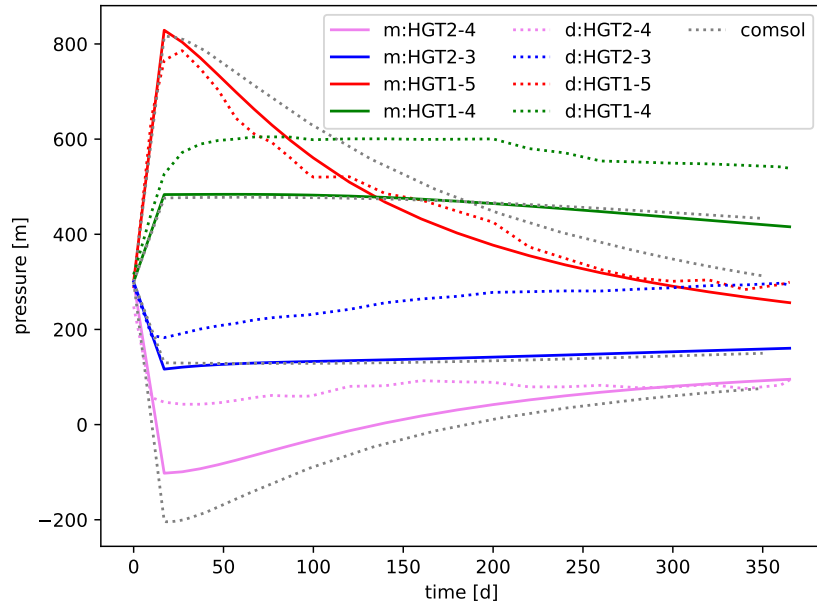


Figure 2: Results of Model 1 – observed pressure.

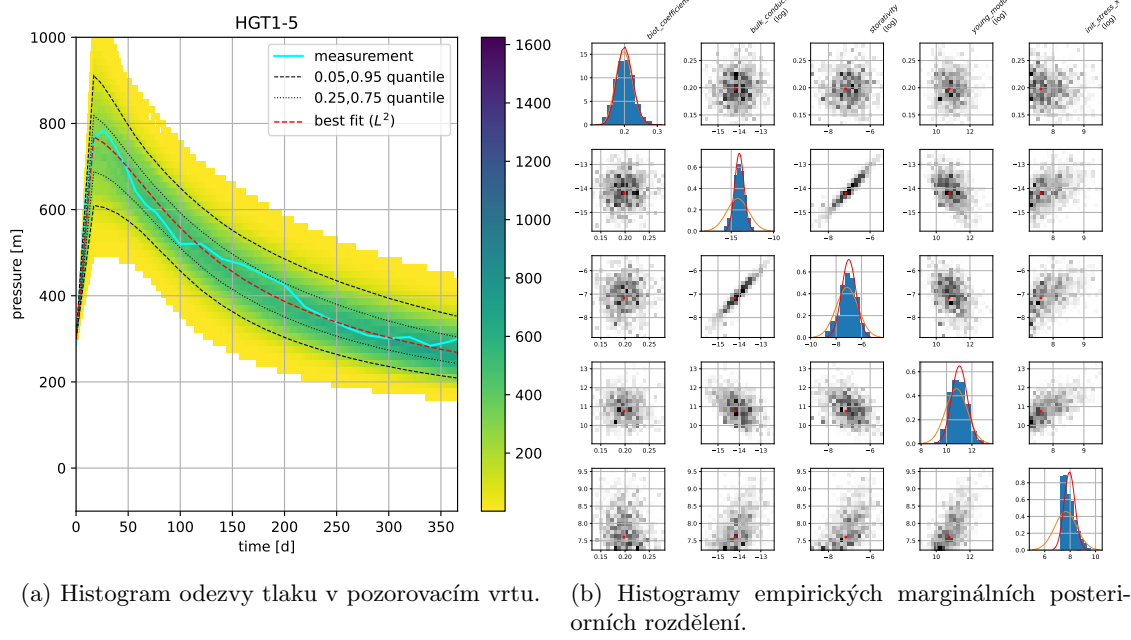


Figure 3: Výsledky pro pozorovací vrt HGT1-5.

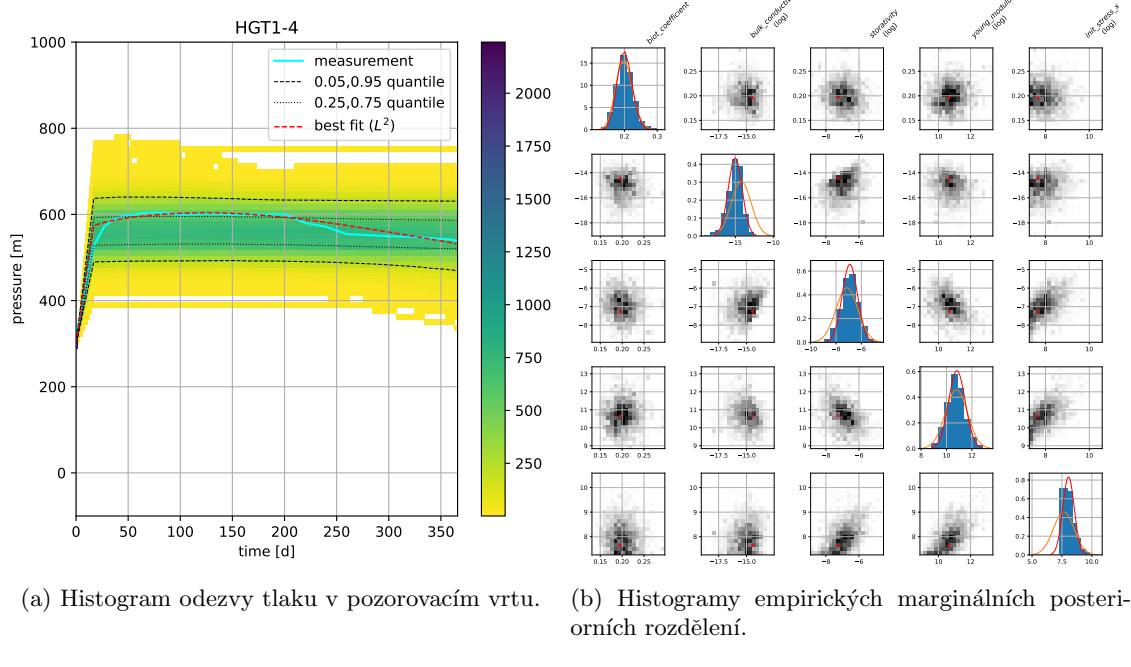


Figure 4: Výsledky pro pozorovací vrt HGT1-4.

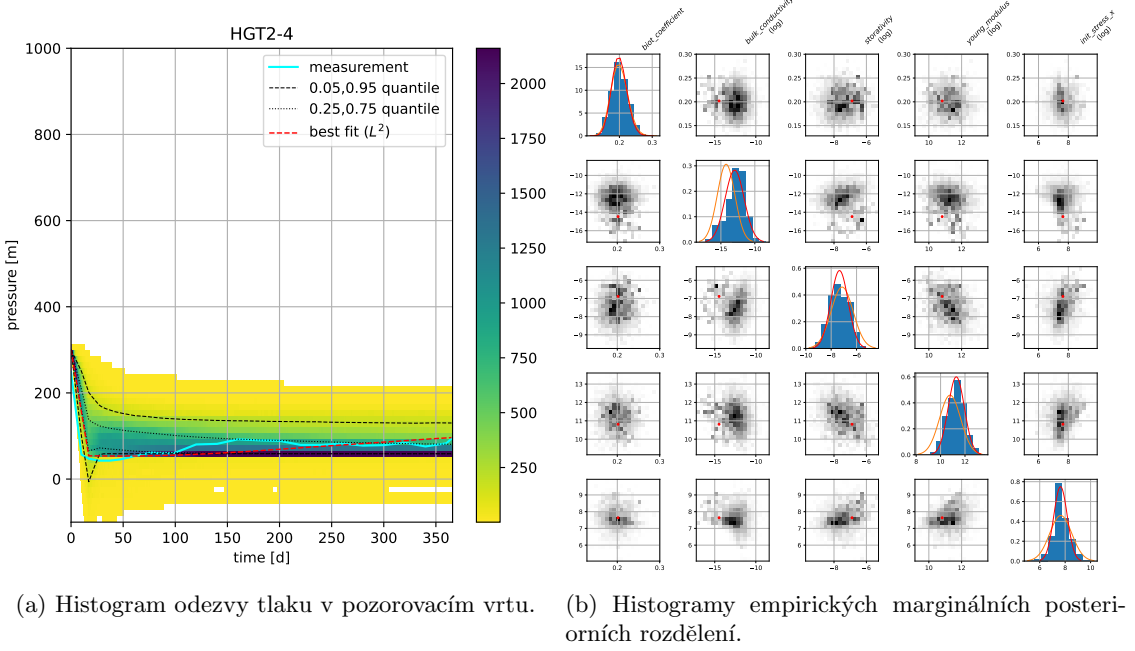


Figure 5: Výsledky pro pozorovací vrt HGT2-3.

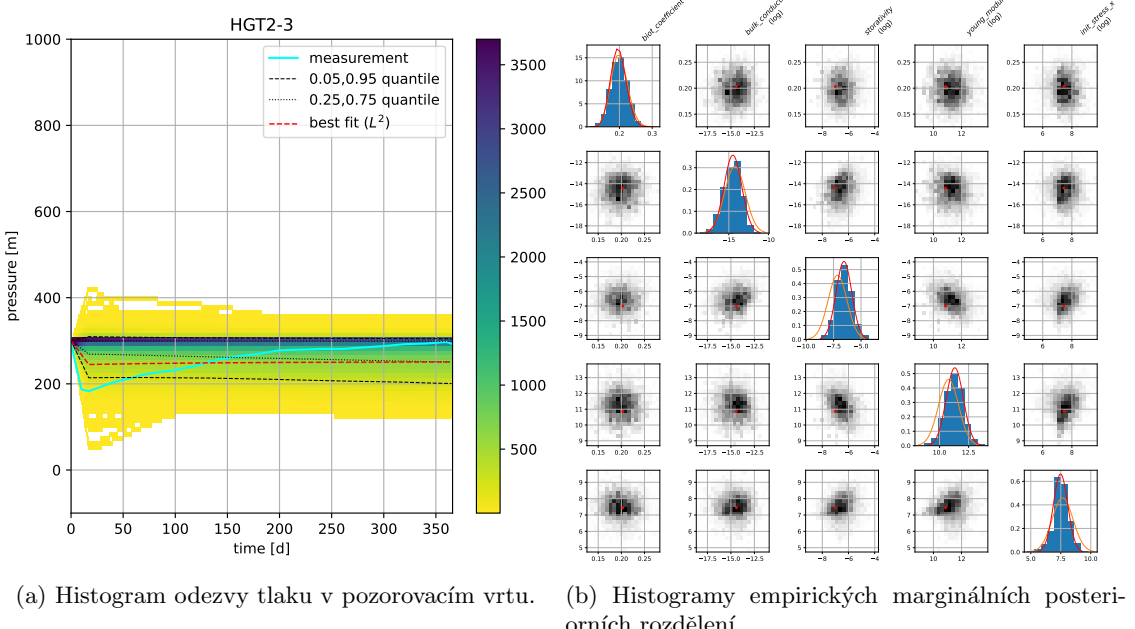


Figure 6: Výsledky pro pozorovací vrt HGT2-4.

0.1.3 Model 2 – nonlinear hydraulic conductivity

The second model is derived directly from Model 1 (Section 0.1.2). We consider the same geometry and parameters with the only difference in hydraulic conductivity.

Nonlinear hydraulic conductivity. Empirical nonlinear dependence of hydraulic conductivity on stress:

$$K = \frac{\rho g}{\mu} \left[\dot{k}_r + \Delta \dot{k}_m \exp(\dot{\beta} \sigma_m) \right] \exp(\dot{\gamma} \Delta \sigma_{VM}) \quad (14)$$

where

- $\dot{k}_r = 2 \cdot 10^{-21} \text{ m}^2$ is *residual (irreducible) permeability at high compressive mean stress* and the fitting constants are: $\Delta \dot{k}_m = 8 \cdot 10^{-17} \text{ m}^2$, $\dot{\beta} = 4 \cdot 10^{-7} \text{ Pa}^{-1}$, $\dot{\gamma} = 3 \cdot 10^{-7} \text{ Pa}^{-1}$

- the mean of the principal stresses, i.e.

$$\sigma_m := \frac{1}{3} \operatorname{tr} \sigma(\mathbf{u}) \quad (15)$$

- von Mises stress

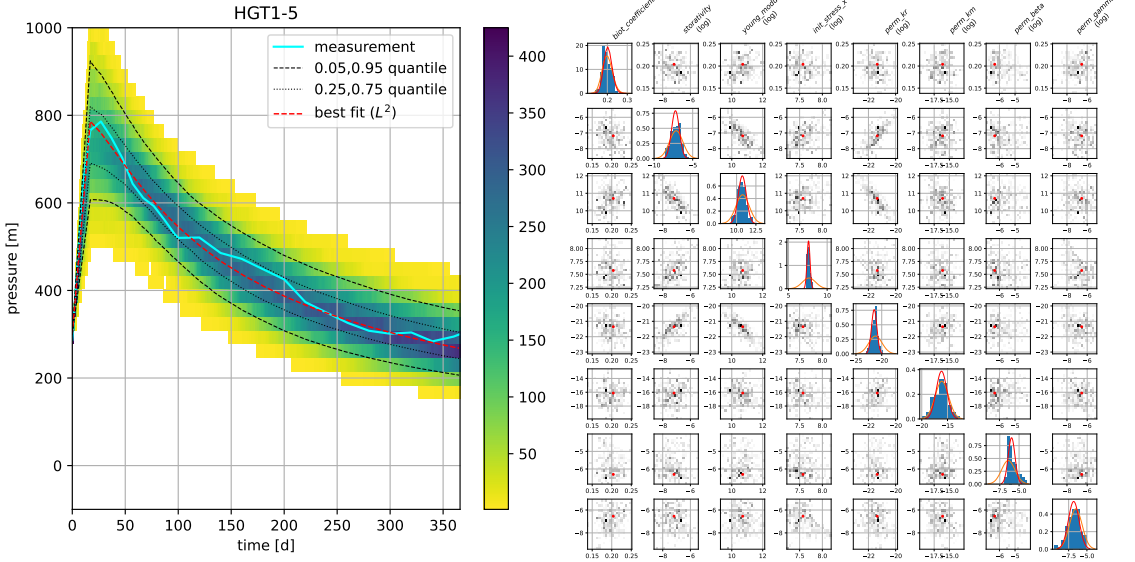
$$\sigma_{VM} := \sqrt{\frac{3}{2} \sigma_d : \sigma_d} = \frac{1}{\sqrt{2}} \sqrt{(\sigma_1 - \sigma_2)^2 + (\sigma_2 - \sigma_3)^2 + (\sigma_1 - \sigma_3)^2}, \quad (16)$$

where $\sigma_d := \sigma(\mathbf{u}) - \frac{1}{3}(\operatorname{tr} \sigma(\mathbf{u}))\mathbb{I}$ is the deviatoric stress;

- $\Delta \sigma_{VM}$ is understood as the *non-negative difference between the computed σ_{VM} and a critical deviatoric stress for onset of shear-induced permeability, σ_c* , by [1]. Let us denote

$$\Delta \sigma_{VM} = \max(0, \sigma_{VM} - \sigma_c), \quad (17)$$

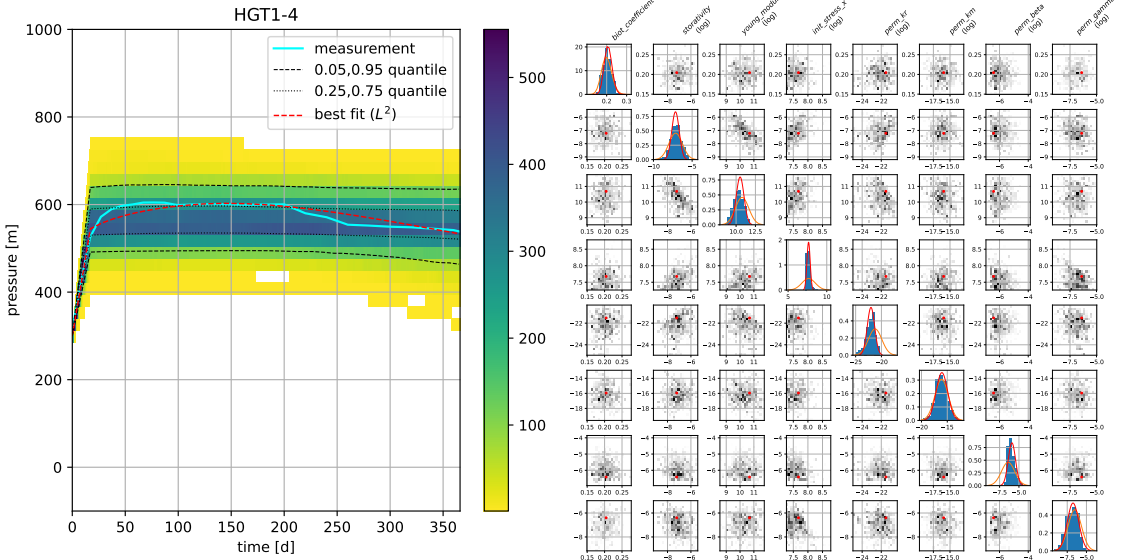
with $\sigma_c = 55 \text{ MPa}$.



(a) Histogram odezvy tlaku v pozorovacim vrtu.

(b) Histogramy empirickych marginálních posteriorních rozdělení.

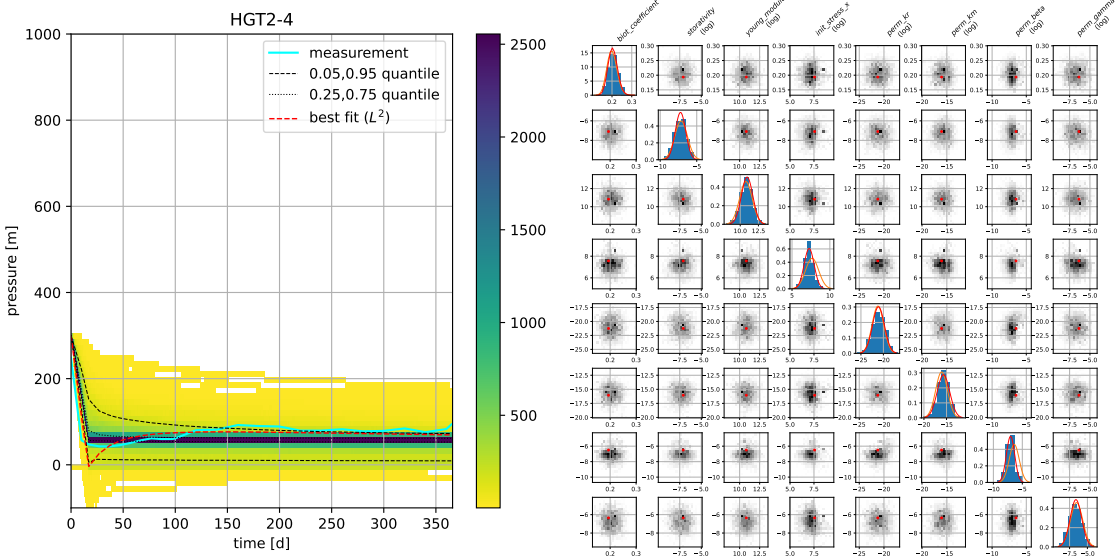
Figure 7: Výsledky pro pozorovací vrt HGT1-5.



(a) Histogram odezvy tlaku v pozorovacim vrtu.

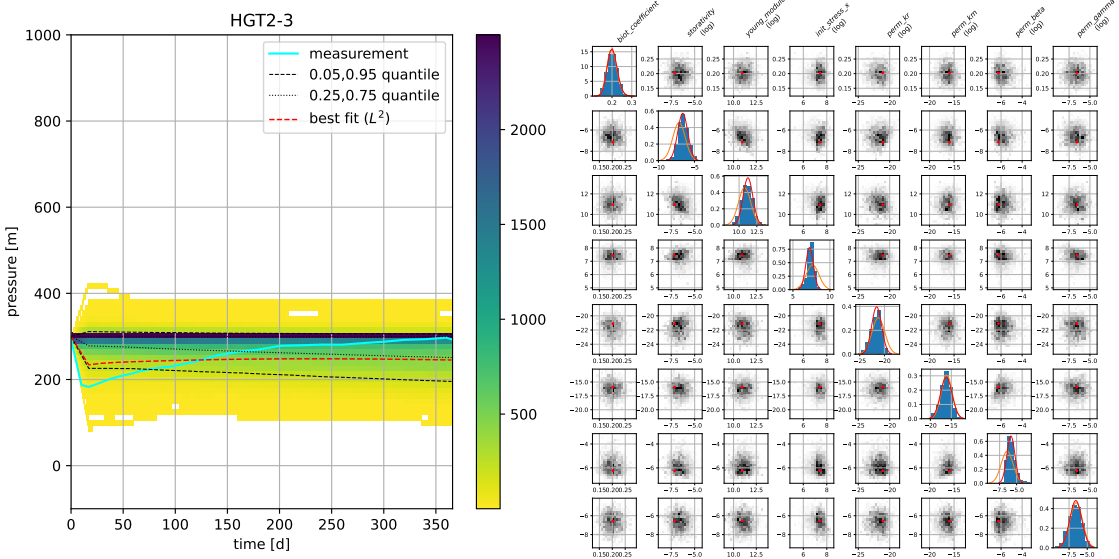
(b) Histogramy empirickych marginálních posteriorních rozdělení.

Figure 8: Výsledky pro pozorovací vrt HGT1-4.



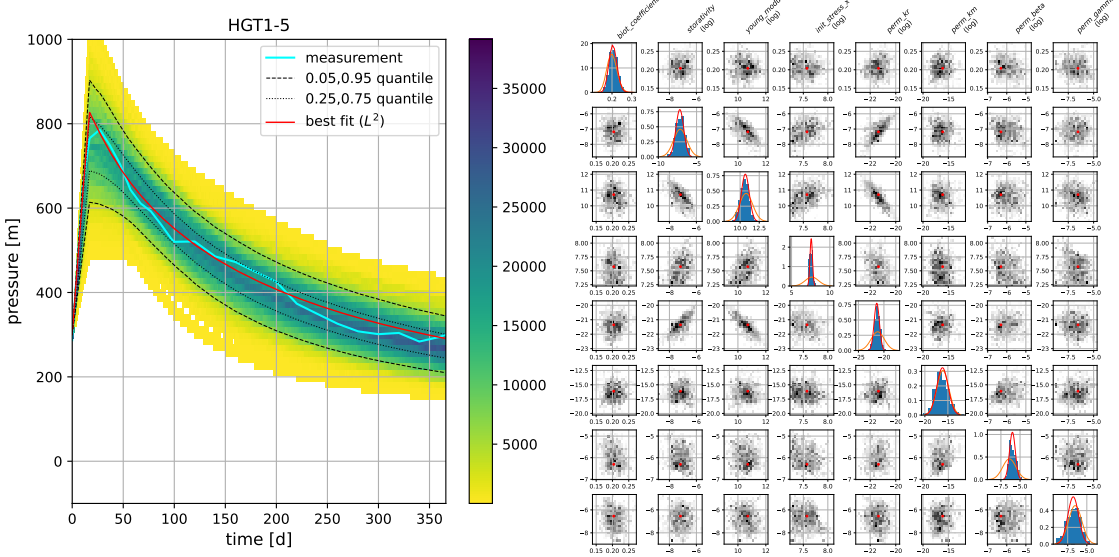
(a) Histogram odezvy tlaku v pozorovacim vrtu. (b) Histogramy empirickych marginálních posteriorních rozdělení.

Figure 9: Výsledky pro pozorovací vrt HGT2-3.



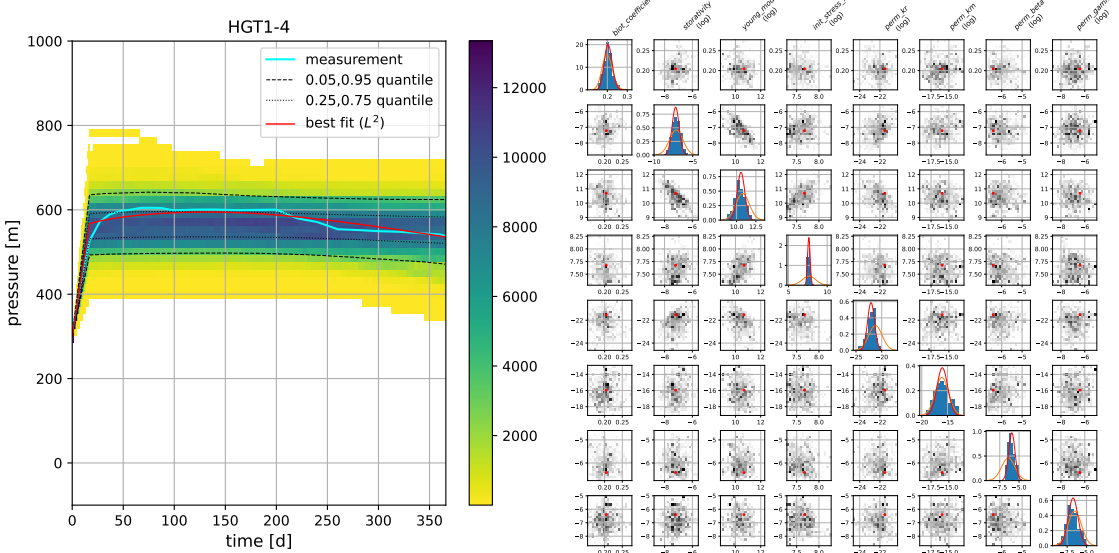
(a) Histogram odezvy tlaku v pozorovacim vrtu. (b) Histogramy empirickych marginálních posteriorních rozdělení.

Figure 10: Výsledky pro pozorovací vrt HGT2-4.



(a) Histogram odezvy tlaku v pozorovacim vrtu. (b) Histogramy empirickych marginálních posteriorních rozdělení.

Figure 11: Výsledky pro pozorovací vrt HGT1-5.



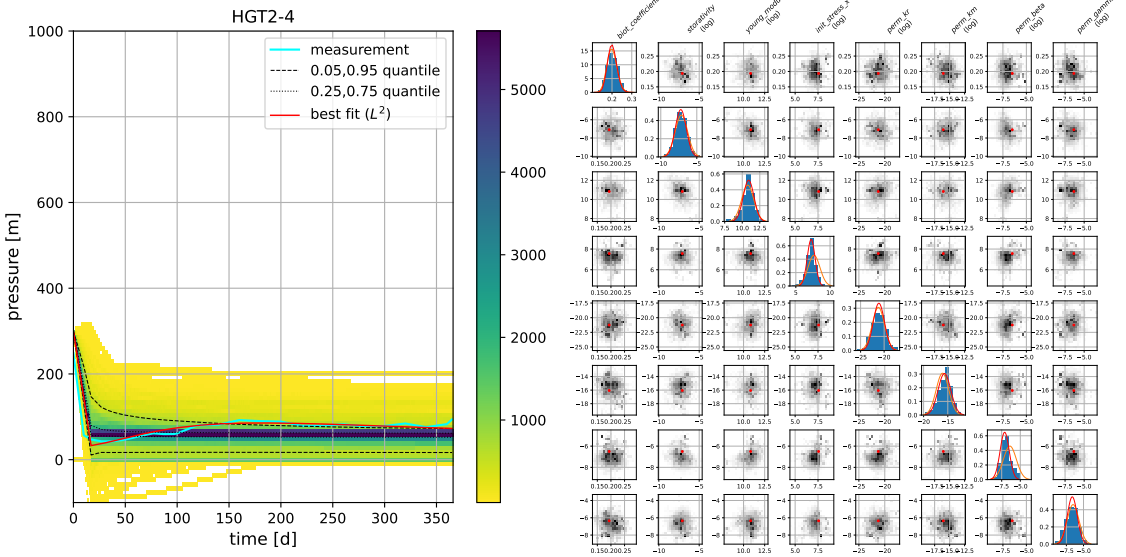
(a) Histogram odezvy tlaku v pozorovacim vrtu. (b) Histogramy empirickych marginálních posteriorních rozdělení.

Figure 12: Výsledky pro pozorovací vrt HGT1-4.

motivace k bayesovi - ziskat vodivost a porozitu, samplu do transportniho modelu - populace bayes dopredny model (rovnice JS), vybrane parametry a volba prioru, navrhove rozdeleni

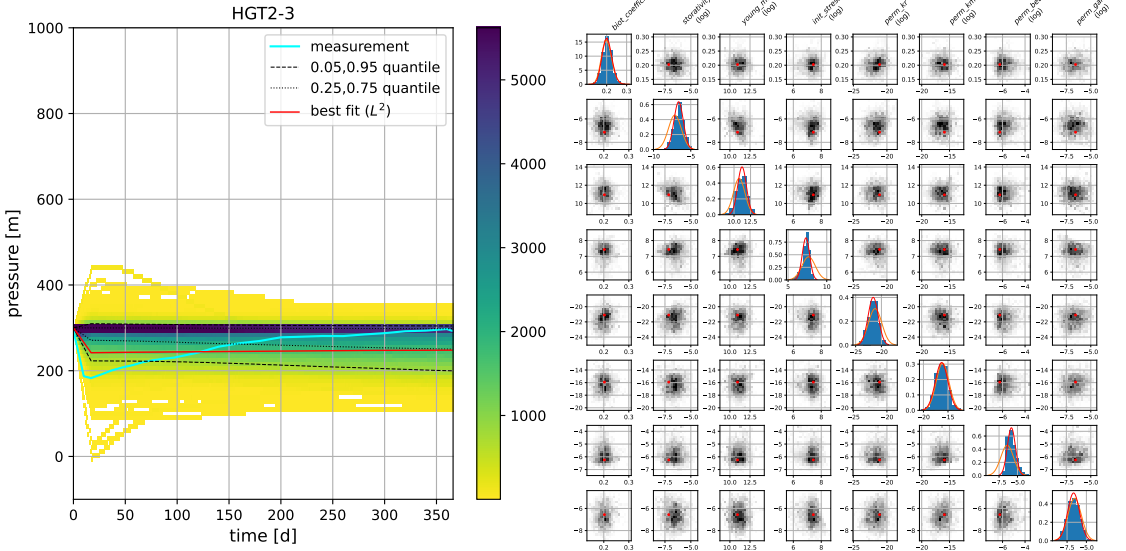
1 Results

In Figure 15 we demonstrate an example visualization of the results by means of marginal histograms. We see the comparison of prior (orange) and posterior (blue) probabilistic distribution



(a) Histogram odezvy tlaku v pozorovacim vrtu. (b) Histogramy empirickych marginálních posteriorních rozdělení.

Figure 13: Výsledky pro pozorovací vrt HGT2-3.



(a) Histogram odezvy tlaku v pozorovacim vrtu. (b) Histogramy empirickych marginálních posteriorních rozdělení.

Figure 14: Výsledky pro pozorovací vrt HGT2-4.

on the diagonal. From the 2D histograms of the parameter pairs we can see significant correlation between hydraulic conductivity and storativity for example and also for pair Young modulus and initial stress i x-axis. The best-fit samples are denoted by red dot.

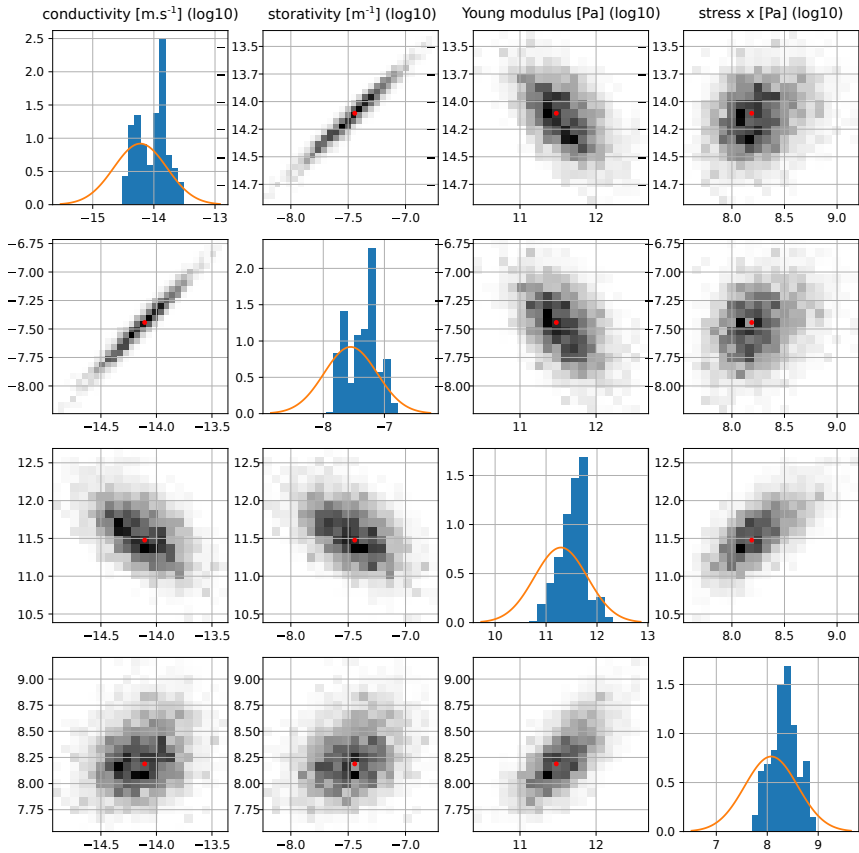


Figure 15: 1D and 2D marginal histograms.

References

- [1] J. Rutqvist. Fractured rock stress-permeability relationships from in situ data and effects of temperature and chemical-mechanical couplings. *Geofluids*, 15(1-2):48–66, 2015. eprint: <https://onlinelibrary.wiley.com/doi/pdf/10.1111/gfl.12089>.